SUPPORTING INFORMATION

A microporous MOF with open metal sites and Lewis basic sites for selective CO_2 capture

Jinjie Qian,*[a‡] Qipeng Li,[b‡] Linfeng Liang,[c] Ting-Ting Li,[d] Yue Hu,*[a] and Shaoming Huang*[a]

[a]*College of Chemistry and Life Science, Zhaotong University, Zhaotong 657000, P. R. China. College of Chemistry and Materials Engineering, Wenzhou University, Wenzhou 325035, P. R. China. E-mail: jinjieqian@wzu.edu.cn; yuehu@wzu.edu.cn; smhuang@wzu.edu.cn; Tel: 86-577-88373064.*

[b]*College of Chemistry and Life Science, Zhaotong University, Zhaotong 657000, P. R. China.*

[c]*State Key Laboratory of Structure Chemistry, Fujian Institute of Research on the Structure of Matter, Chinese Academy of Sciences, Fuzhou, Fujian 350002, China.*

[d]*Research Center of Applied Solid State Chemistry, Ningbo University, Ningbo, 315211, P. R. China.*

**To whom correspondence should be addressed: E-mail: jinjieqian@wzu.edu.cn; yuehu@wzu.edu.cn; smhuang@wzu.edu.cn; Tel: 86-577-88373064.*

‡ *These authors contributed equally.*

Table of Content

S1. Materials and Methods

1.1. Materials and Instruments.

All the reactants are of reagent-grade quality and used as purchased commercially without further purification. All the reactions were carried out in approximately 23 ml glass vials under the autogenous pressure. The powder X-ray diffraction patterns (PXRD) were collected by a Bruker D8 Advance using Cu Kαradiation (λ = 0.154 nm). Single component gas adsorption measurements were performed in the Accelerated Surface Area and Porosimetry 2020 System (ASAP2020). Elemental analyses for C, H, N were carried out on a German Elementary Vario EL III instrument. Thermogravimetric analyses (TGA) were recorded on a NETZSCH STA 449C unit at a heating rate of 10 $^{o}C\cdot min^{-1}$ under flowing nitrogen atmosphere. Field-emission scanning electron microscopy (FE-SEM) images were obtained on a Nova NanoSEM200 scanning electron microscope.

1.2. Synthesis of $[In_3O(BQDC)_3(MeOH)_3](NO_3)\bullet$DMA (InOF-15)

A mixture of $In(NO_3)_3$ (0.10 mmol, 33 mg) and H_2BQDC (0.06 mmol, 20 mg, H_2BQDC = 2,2‘-biquinoline-4,4‘-dicarboxylic acid) in DMA (3 ml), dioxane (3 ml) and MeOH (1 ml) with an additional HNO_3 (0.01 ml 65 wt%) was sealed in a 23 ml glass vial, which was heated at 85 ^{o}C for 5 days, then cooled down to room temperature. It is worth pointing there are disordered charge-balancing NO_3^- counter anions existing inside the solvent-accessible void, which has been subtracted from the reflection data by the SQUEEZE method as implanted in PLATON program. After washed by fresh DMA, the colorless stick-like crystals of **InOF-15** were obtained in *ca*. ~47% yield based on the organic ligand H_2BQDC. Elemental analysis was calculated for **InOF-15**: C, 51.33%; H, 3.086%; N, 6.23%. Found: C, 51.05%; H, 3.098%; N, 6.24%. The phase purity of the sample was also confirmed by PXRD (Figure. S6).

1.3. Single-Crystal X-ray Crystallography

The structure data of **InOF-15** was collected on a SuperNova, Dual, Cu at zero, Atlas diffractometer. The crystal was kept at 99.99(16) K during data collection. By using Olex2,[S1] the structure was solved with the ShelXS[S2] structure solution program using Direct Methods and refined with the ShelXL[S3] refinement package using Least Squares minimisation. Crystallographic data and structure refinement parameters for this crystal is summarized in Table S1. We employed PLATON/SQUEEZE[S4] to calculate the contribution to the diffraction from the solvent region and

thereby produced a set of solvent-free diffraction intensities. The coordinated O^{2-} and NO_3^- in this structure are determined according to charge balance and a rational experimental bond and angle parameters which are well consistent with the experimental data ever reported.[S5] The final formula was calculated from the SQUEEZE results combined with elemental analysis data and TGA data. More details on the crystallographic studies as well as atomic displacement parameters are given in Supporting Information as CIF files. Crystallographic data for the structure reported in this paper has been deposited. The following crystal structure has been deposited at the Cambridge Crystallographic Data Centre and allocated the deposition number (CCDC No.1554960) for **InOF-15**. These data can be obtained free of charge via *www.ccdc.cam.ac.uk/data_request/ cif.*

Table S1 Summary of Crystal Data and Refinement Results

Items	**InOF-15**
formula	$C_{63}H_{39}In_3N_6O_{16}$
Mass	1480.46
crystal system	Hexagonal
space group	*P*63/m
a (Å)	15.1951(11)
b (Å)	15.1951(11)
c (Å)	23.091(2)
α (°)	90.00
β (°)	90.00
γ (°)	120.00
V (Å^3)	4617.2(7)
T (K)	296(2)
Z	12
F(000)	1468.0
GOF	0.1128
R_1 (I>2σ(I))	0.0402
wR_2 (all reflections)	0.1330

InOF denotes Indium-Organic Framework; More details see CIF files.

S2. Additional X-ray Crystal Structural Figures

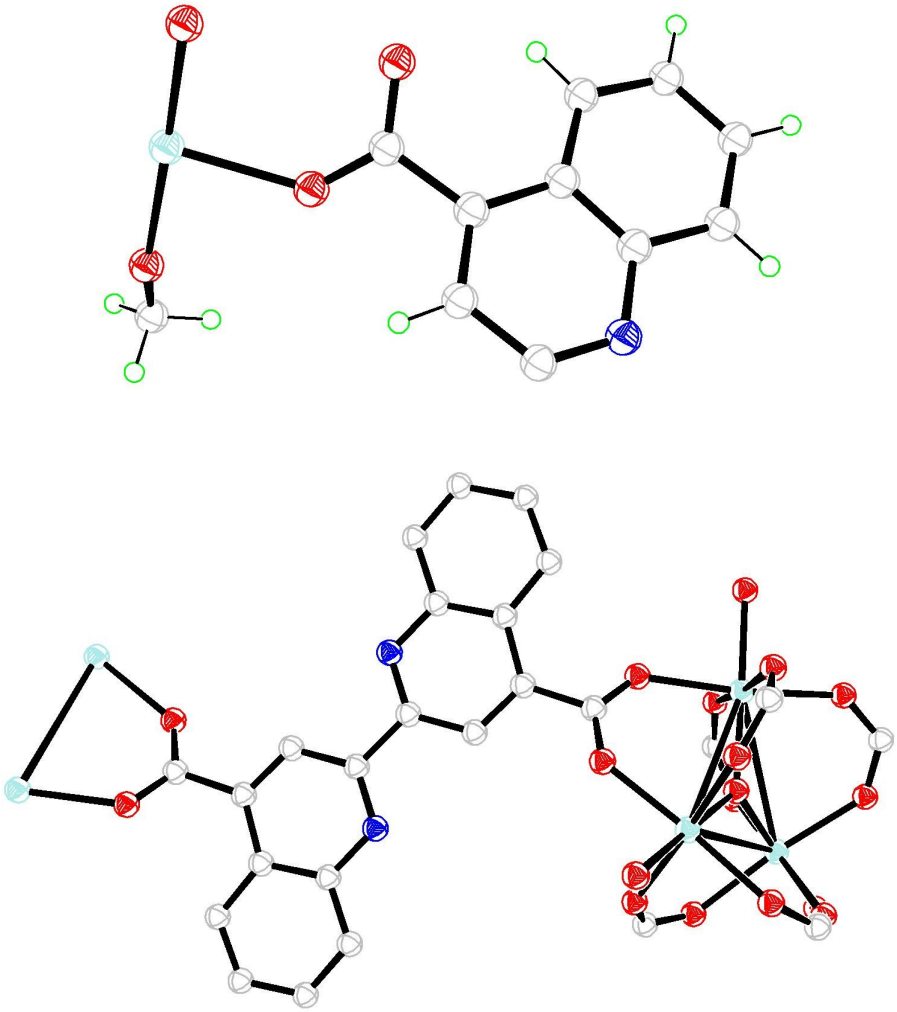

Figure S1. The asymmetric unit (up) and the coordination environment of In(III) and $BQDC^{2-}$ ligand (down) in **InOF-15**.

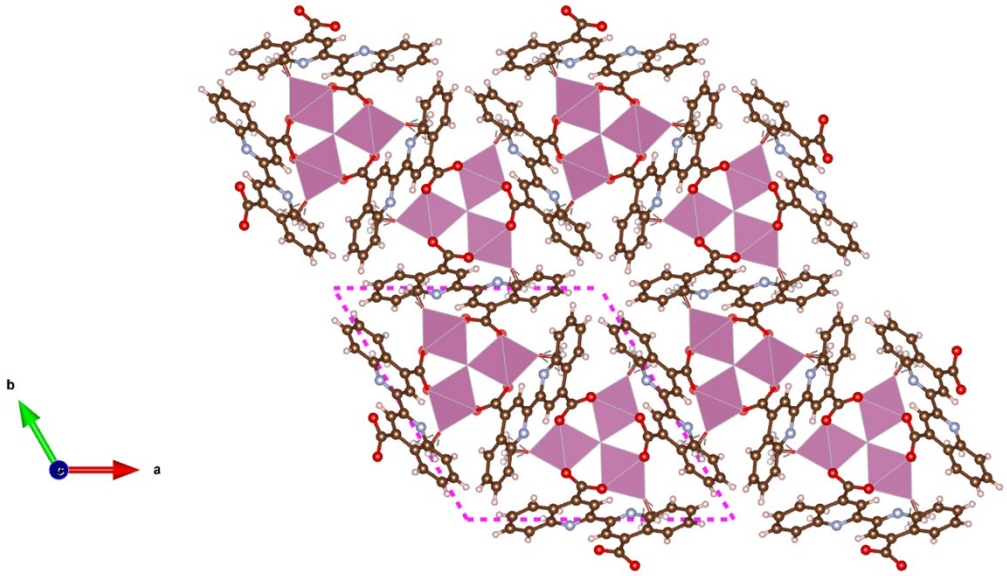

Figure S2. The single crystal structure of **InOF-15** viewed along *c*-axis, in which the dashed line represents the unit cell.

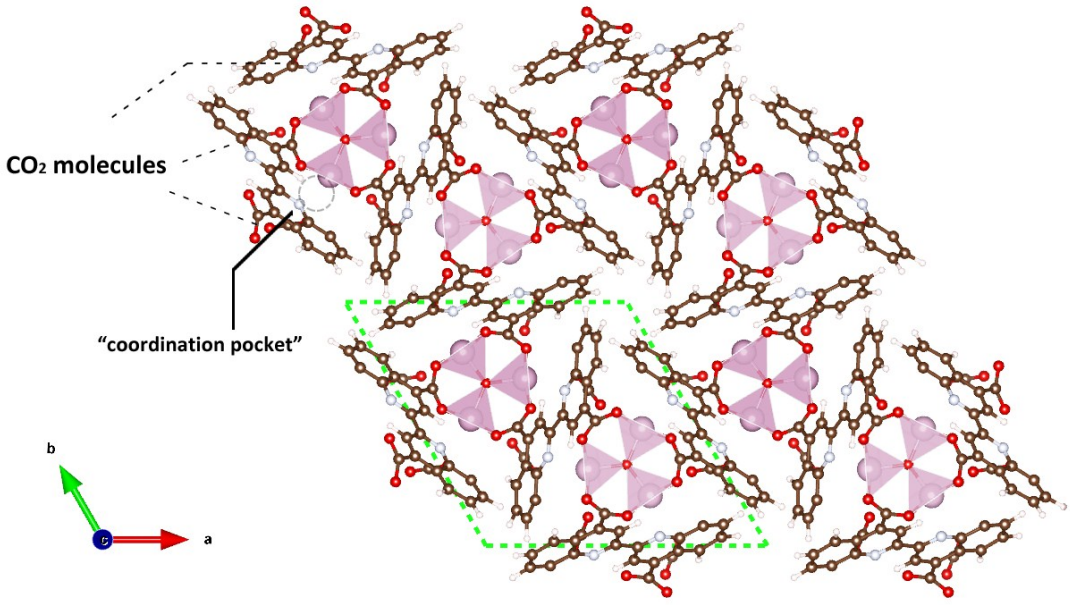

Figure S3. The optimized crystal structure of **InOF-15·CO_2** viewed along *c*-axis, in which the dashed line represents the unit cell. The captured CO2 molecules are inclined to be encapsulated to the coordination pocket between OMSs and LBSs

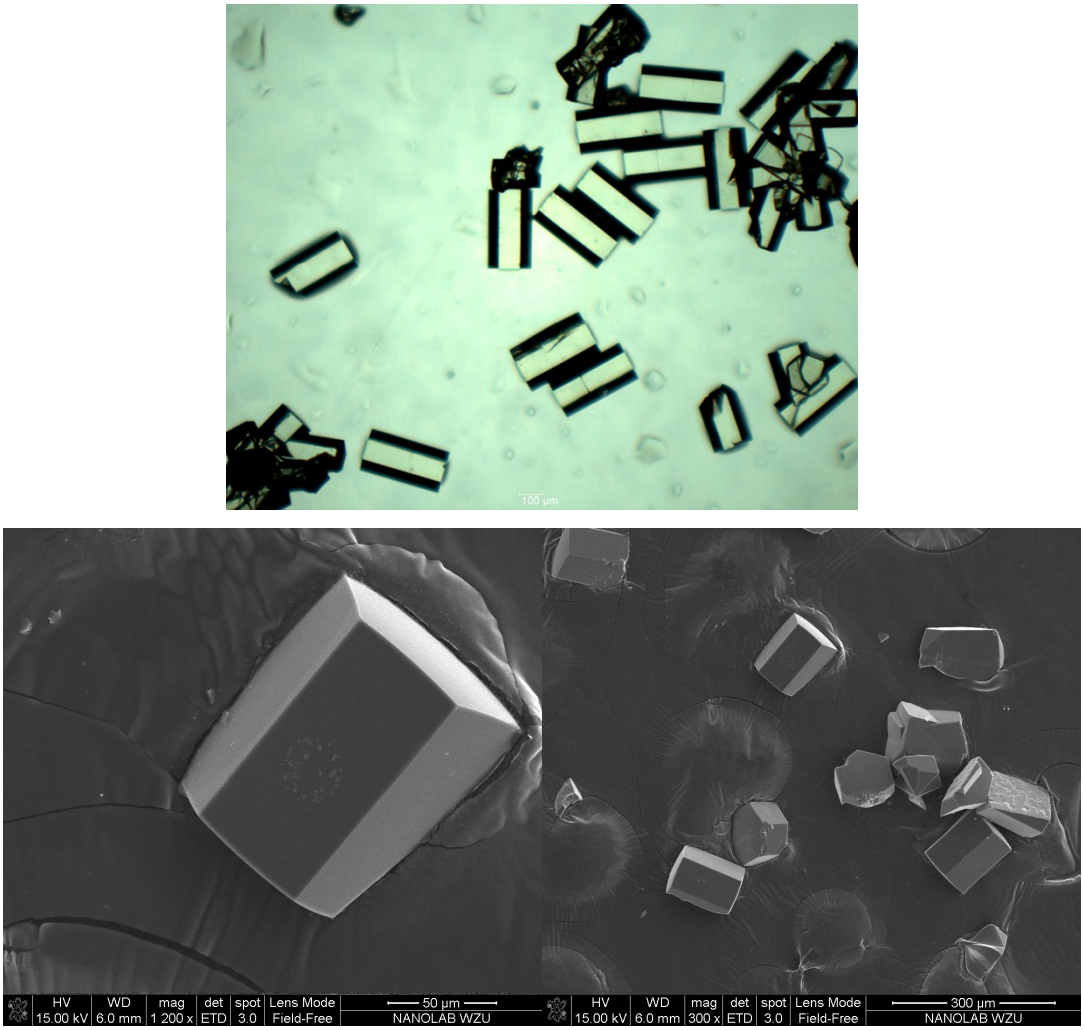

Figure S4. The single crystals photographs (top) and SEM images (bottom) of **InOF-15**.

S3. Topological Analysis

Topology for **InOF-15**

$[In_3O(CO_2)_6]$ SBU links by bridge ligands and has

Common vertex with					R(A-A)	
SBU	0.6667	1.3333	0.2500	(1 2-1)	14.500A	1
SBU	0.6667	1.3333	1.2500	(1 2 0)	14.500A	1
SBU	-0.3333	0.3333	0.2500	(0 1-1)	14.500A	1
SBU	-0.3333	0.3333	1.2500	(0 1 0)	14.500A	1
SBU	0.6667	0.3333	0.2500	(1 1-1)	14.500A	1
SBU	0.6667	0.3333	1.2500	(1 1 0)	14.500A	1

Structure consists of 3D framework with $[In_3O(CO_2)_6]$ SBU

Coordination sequences

SBU:	1	2	3	4	5	6	7	8	9	10
Num	6	20	42	74	114	164	222	290	366	452
Cum	7	27	69	143	257	421	643	933	1299	1751

TD10=1751

Vertex symbols for selected sublattice

$[In_3O(CO_2)_6]$ SBU Point (Schlafli) symbol:{4^9.6^6}

Extended point symbol:[4.4.4.4.4.4.4(2).4(2).4(2).6(8).6(8).6(8).6(8).6(8).6(8)]

Point (Schlafli) symbol for net: **{4^9.6^6}**

6-c net; uninodal net

Topological type: **acs**; 6/4/h2 (topos&RCSR.ttd) {4^9.6^6}-VS [4.4.4.4.4.4.4(2).4(2).4(2).6(4).6(4).6(4).6(4).6(4).6(4)] (71251 types in 10 databases)

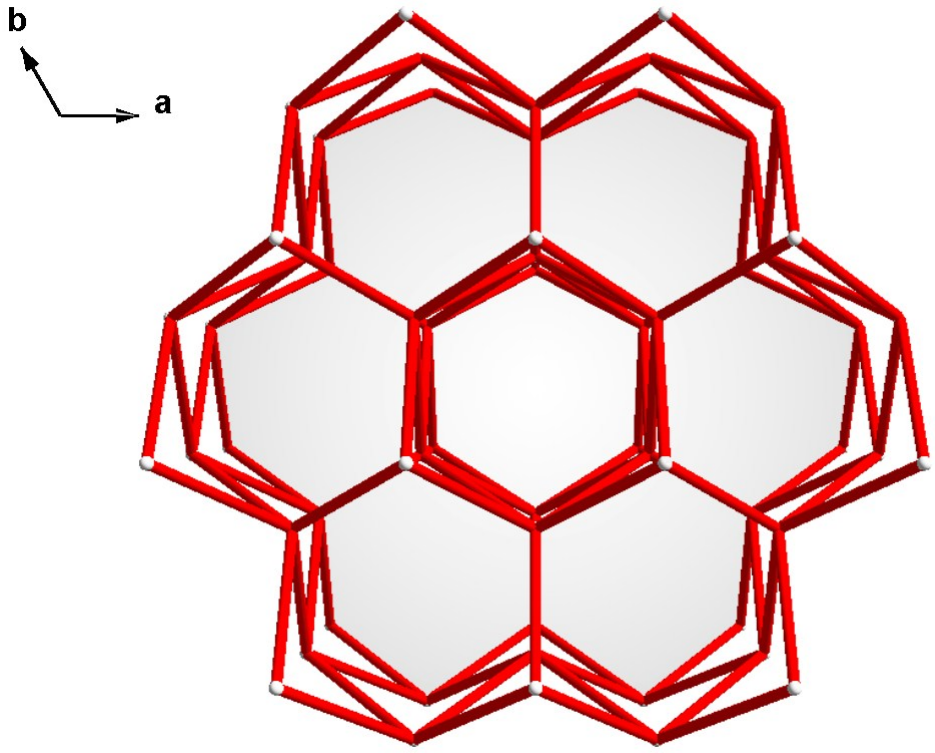

Figure S5. The 3-dimensional ***acs*** network of **InOF-15**.

S4. PXRD Data

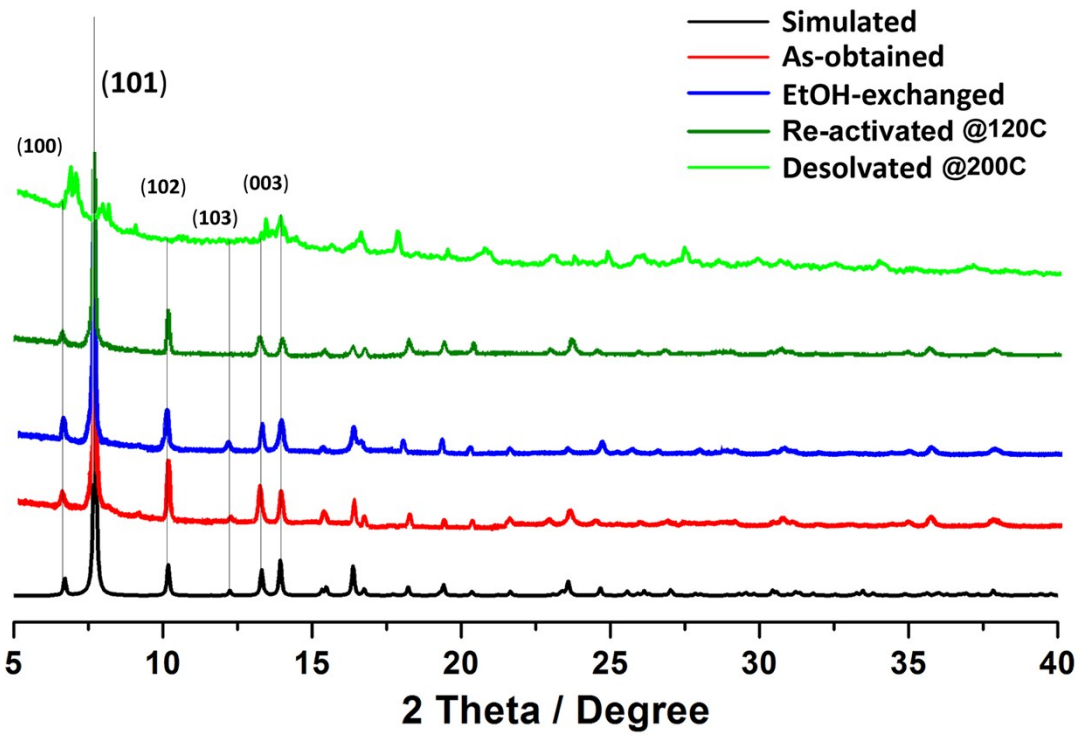

Figure S6. PXRD patterns of **InOF-15**: simulated from the crystallographic information file (black, bottom); from the as-prepared sample (red); from the EtOH-exchanged sample (blue); from the desolvated sample at 120 °C (olive), from the desolvated sample at 200 °C (green, top).

In this case, **InOF-15** actually is a 3-dimensional flexible MOF with *acs* network, which is topologically identical to a well-known flexible MIL-88B(Fe). It is no doubt that the flexibility of this MOF can be affected when heated to a higher activation temperature. Initially, from the TGA curve (Figure S7) we took 200 °C to fully desolvate our as-obtained crystalline materials, whose phase turned out to be different structural PXRD pattern (Figure S6, green line), especially below 2-theta of 15°, which indicated the structural decomposition to some extent with some broad peaks.

Now, we take a lower activation temperature to re-desolvate our samples at 120 °C for 10 hours under vacuum, which showed the sharp PXRD peaks confirming the desolvated sample retained the crystalline ordered structure in long range.

S5. TGA data and Analysis

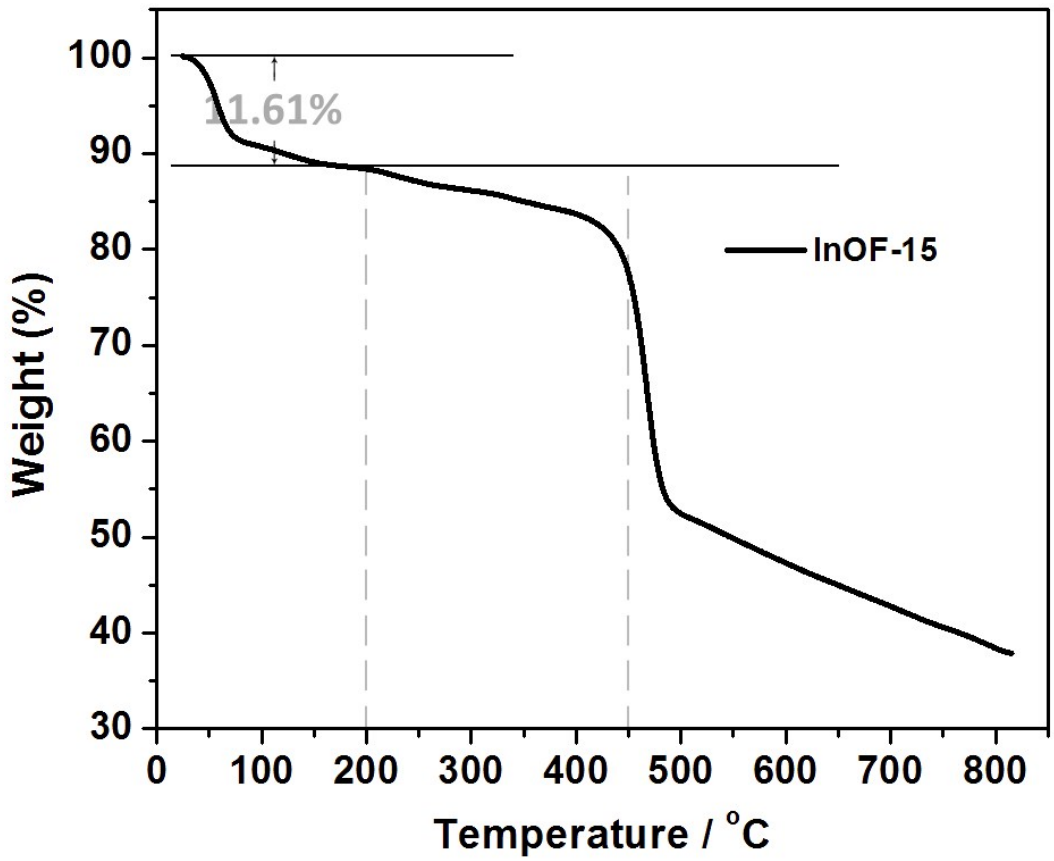

Figure S7. TGA curve for **InOF-15** samples.

Thermogravimetric analysis (TGA) measurements of **InOF-15** is conducted in the temperature range of 30-800 °C under a flow of nitrogen with the heating rate of 10°C min^{-1}. **InOF-15** shows a weight loss of ca. 11.61% from 25-200 °C, which can be reasonably attributed to the loss of three MeOH molecules and one guest DMA molecule (calcd 11.68%), and then the main framework begins to quickly collapses upon further heating @ 450 °C (Figure S7). Its final formula of **InOF-15** with guest solvent molecules were calculated from the SQUEEZE results and combined with the TGA and elemental analysis data.

S6. Computational Details and Sorption Analyses

To investigate the theoretical N_2 adsorption in **InOF-15**, the Grand canonical Monte Carlo (GCMC) simulations were carried out using the Sorption module of Materials Studio 8.0 package.[S6] The materials in the simulation were modeled as rigid structures, which ignores the skeleton stretching and bending vibration. The number of unit cells in the simulation box is 2×2×2 and periodic boundary conditions were applied in all directions. The Dreiding force field was used and the charges calculated *via* the Q_{eq} charge equilibration. In GCMC simulations, chemical potentials obtained by Peng-Robinson equation of state were taken as inputs to calculate the gas adsorption. To further investigate interactions between CO_2 molecules and the **InOF-15**, the Dmol3 module in Materials studio 8.0 were used to predict the best binding sites of CO_2 molecules onto the frameworks.[S6]

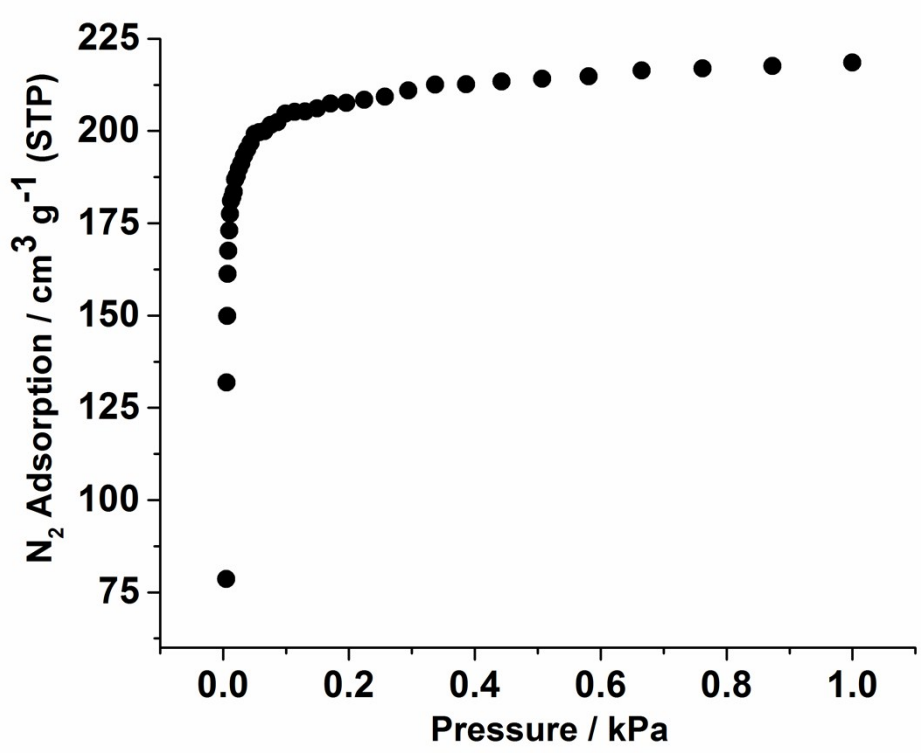

Figure S8 The simulation of N_2 isotherm at 77 K in **InOF-15**.

N_2, CH_4 and CO_2 Isotherms.

All the N_2, CH_4 and CO_2 isotherms for **InOF-15** were determined using an IGA gravimetric adsorption apparatus at the Wenzhou University in a clean ultra high vacuum system. Before measurements, about 100 mg solvent-exchanged samples were loaded into the sample basket within the adsorption instrument (ASAP 2020) and then degassed under dynamic vacuum at 100 °C for 10 h to obtain the fully desolvated samples. The N_2 sorption measurement was performed at 77 K; the CO_2 and CH_4 sorption measurement was performed at 273 and 295 K.

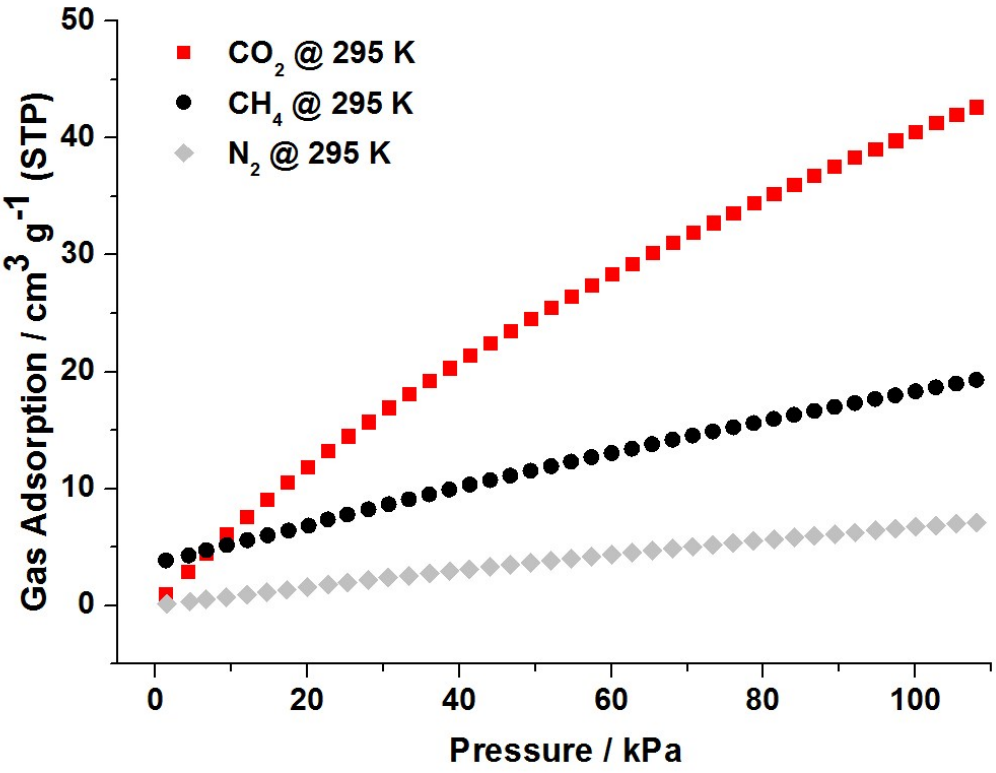

Figure S9. The simulation of N_2 isotherm at 77 K in **InOF-15**.

S7. The Heat of Adsorption for CO_2

CO_2 isotherms (adsorption and desorption) measured at 273 and 295 K for **A InOF-15** were fitted to the following Equation 1.

The adsorption isothere is represented by[S7]

$$\ln (P/P_0) = q_i/RT + C \qquad (1)$$

where

q_i = isosteric heat of adsorption

C = unknown constant

The isosteric heat of adsorption, q_i is determined by finding the slope of $\ln (P/P_0)$ as a function of 1/RT for a set of isotherms measured at different temperatures.

y=ln(x)+1/k*(a0+a1*x+a2*x^2+a3*x^3+a4*x^4+a5*x^5)+(b0+b1*x+b2*x^2)

InOF-15		Value	Standard Error
ln(P)	a0*	-3738.51328	5.96884
	a1*	5.78066	0.27716
	a2*	-0.05381	0.00331
	a3*	2.41759E-4	2.67142E-5
	a4*	-1.31442E-6	1.87897E-7
	a5*	2.82434E-9	4.79717E-10
	b0*	14.32332	0.02056
	b1*	-0.00914	9.3437E-4
	b2*	1.02694E-4	9.37979E-6
	k	273	0
	k	295	0

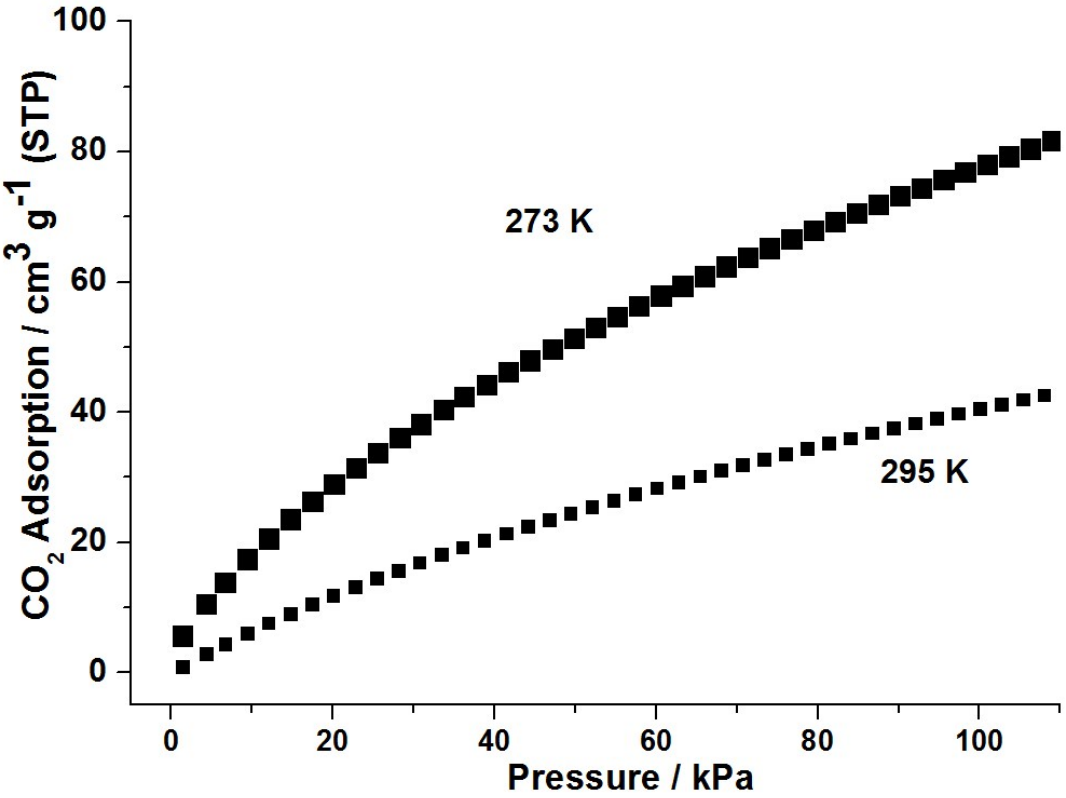

Figure S10. CO_2 isotherm at 273 and 295 K in **InOF-15**.

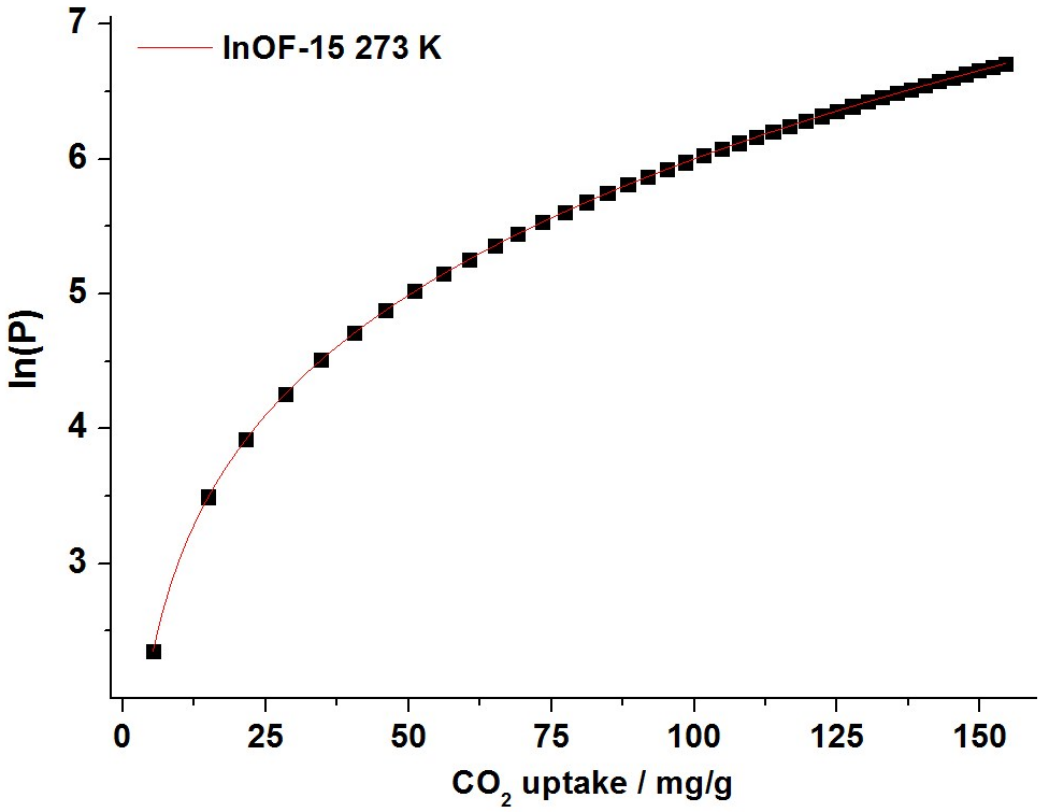

Figure S11. Nonlinear curve fitting of CO_2 adsorption isotherm for **InOF-15** at 273 K.

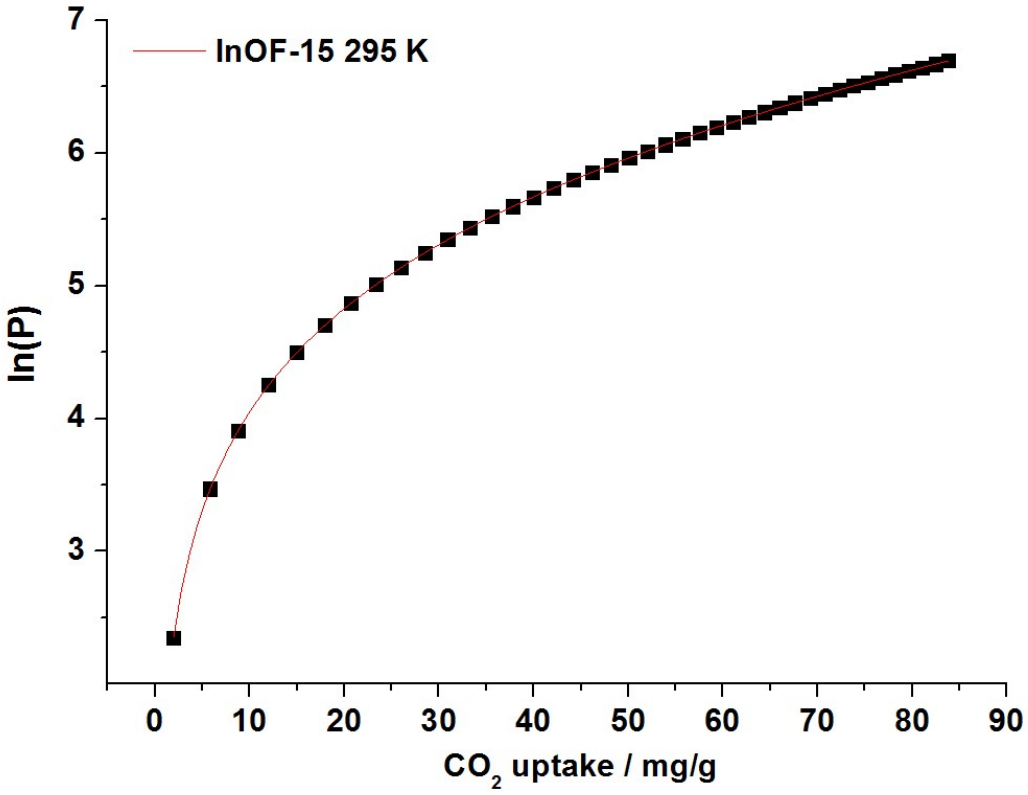

Figure S12. Nonlinear curve fitting of CO_2 adsorption isotherm for **InOF-15** at 295 K.

S7 References

[S1] O. V. Dolomanov, L. J. Bourhis, R. J. Gildea, J. A. K. Howard and H. Puschmann, *J. Appl. Cryst*. **2009**, *42*, 339.

[S2] SHELXS, G.M. Sheldrick, *Acta Cryst*. **2008**, *A64*, 112.

[S3] SHELXL, G.M. Sheldrick, *Acta Cryst*. **2008**, *A64*, 112.

[S4] (a) A. L. Spek, *J. Appl. Crystallogr.* **2003**, *36*, 7; (b) P. v.d. Sluis and A. L. Spek, *Acta Crystallogr., Sect. A*, **1990**, *46*, 194.

[S5] (a) Q. R. Fang, G. S. Zhu, M. Xue, J. Y. Sun, F. X. Sun, S. L. Qiu, Inorg. Chem. **2006**, *45*, 3582; (b) J. H. He, Y. T. Zhang, Q. H. Pan, J. H. Yu, H. Ding, R. R. Xu, Micro. Meso. Mater. **2006**, *90*, 145; (c) S. Zheng, T. Wu, J. Zhang, M. Chow, R. A. Nieto, P. Feng, X. Bu, Angew. Chem. Int. Ed. **2010**, *49*, 5362; (d) X. -R. Hao, X. -L. Wang, K. -Z. Shao, G. -S. Yang, Z. -M. Su, G. Yuan, CrystEngComm., **2012**, *14*, 5596; (e) H. -L. Li, M. Eddaoudi, M. O'Keeffe, O. M. Yaghi, Nature, **1999**, *402*, 276.

[S6] a) J. B. Hu, J. Liu, Y. Liu and X. Yang, J. Phys. Chem. C., **2016**, 120, 10311-10319; b) Y. Liu, H. L. Li and J. Liu, Fuel., **2016**, 184, 474-480; c) S. H. Yang, J. L. Sun, A. J. Ramirez-Cuesta, S. K. Callear, W. I. F. David, D. P. Anderson, R. Newby, A. J. Blake, J. E. Parker, C. C. Tang and M. Schröder, Nature Chemistry., **2012**, 4, 887-894; d) Accelrys, Materials Studio Getting Started, release 8.0; Accelrys Software, Inc.: San Diego, CA, **2012**.

[S7] ASAP 2020 Accelerated Surface Area and Porosimetry System Operator's Manual V4.00, Appendix C, C-43.